Journal of Sensor Science and Technology
Vol. 28, No. 2 (2019) pp. 81-87
http://dx.doi.org/10.5369/JSST.2019.28.2.81
pISSN 1225-5475/eISSN 2093-7563

Constraint-Combined Adaptive Complementary Filter for Accurate Yaw Estimation in Magnetically Disturbed Environments

Woo Chang Jung and Jung Keun Lee+

Abstract

One of the major issues in inertial and magnetic measurement unit (IMMU)-based 3D orientation estimation is compensation for magnetic disturbances in magnetometer signals, as the magnetic disturbance is a major cause of inaccurate yaw estimation. In the proposed approach, a kinematic constraint is used to provide a measurement equation in addition to the accelerometer and magnetometer signals to mitigate the disturbance effect on the orientation estimation. Although a Kalman filter (KF) is the most popular framework for IMMU-based orientation estimation, a complementary filter (CF) has its own advantages over KF in terms of mathematical simplicity and ease of implementation. Accordingly, this paper introduces a quaternion-based CF with a constraint-combined correction equation. Furthermore, the weight of the constraint relative to the magnetometer signal is adjusted to adapt to magnetic environments to optimally deal with the magnetic disturbance. In the results of our validation experiments, the average and maximum of yaw errors were 1.17° and 1.65° from the proposed CF, respectively, and 8.88° and 14.73° from the conventional CF, respectively, showing the superiority of the proposed approach.

Keywords: Yaw estimation, Kinematic constraint, Adaptive complementary filter, Magnetic disturbance

1. INTRODUCTION

Inertial and magnetic measurement unit (IMMU)-based 3D orientation estimation has a variety of applications mainly because it has no measurement volume limitation [1-3]. Typically, an IMMU consists of a triaxial gyroscope, accelerometer, and magnetometer. The IMMU estimates 3D orientation using the complementary relationships among the three sensors. The gyroscope provides angular velocity for prediction and the accelerometer and magnetometer provide vertical and horizontal references for correction [4-5].

However, there are two difficulties in the correction process. First, accelerometer signals contain external acceleration as well as gravity (which is the vertical reference vector) under dynamic conditions, making it difficult to use the accurate vertical reference [6]. Second, magnetometer signals can be easily disturbed by inhomogeneous magnetic fields from any magnetic materials in the vicinity of the sensor. It is generally considered that the second difficulty is more problematic than the first in outdoor applications [7-9].

Orientation estimation methods with magnetic disturbance compensation mechanisms have been proposed to improve the accuracy of yaw estimation. Bachmann *et al.* [10] and Madgwick *et al.* [11] proposed a blend of the angular velocity-integrated orientation using gyroscope signals and an optimization technique-derived orientation using accelerometer and magnetometer signals. Lee and Park [12] proposed a method of selectively using the reference vectors according to the magnitudes of external acceleration and magnetic disturbances by setting thresholds. This technique avoids disturbances that cause adverse effects. Furthermore, the magnetic disturbance has been designated as a state in the Kalman filter through a Markov chain model, in order to actively compensate for the disturbance by estimating it [13-15]. However, the Markov chain model is based on a type of random walk, not on a robust measurement. This is a fundamental limitation of the model-based approaches.

In this paper, a kinematic constraint is used to provide an additional measurement equation in addition to the accelerometer and magnetometer signals, and thus to mitigate the disturbance's effect on the orientation estimation. In most systems that require 3D orientation information, such as the human body or

Dept. of Mechanical Eng., Hankyong National Univ.
327 Jungang-ro, Anseong, Gyeonggi 456-749, Korea.
+Corresponding author: jklee@hknu.ac.kr
(Received: Mar. 9, 2019, Revised: Mar. 27, 2019, Accepted: Mar. 28, 2019)

manipulators, segments or links are connected by joints. In particular, this research deals with a kinematic constraint generated by a spherical joint by considering that many mechanical joints are rotational joints that allow only relative rotations, like the spherical joint.

In the literature, the constraint has been used mainly to improve the joint angle estimation accuracy [16-18]. Choi and Lee [19] showed that the constraint can be used to improve tilt estimation rather than joint angles.

In terms of a type of filter in which orientation estimation algorithms are implemented, a Kalman filter (KF) is the most popular framework for IMMU-based orientation estimation because of its optimal and recursive characteristics. However, a complementary filter (CF) has its own advantages over KF in terms of mathematical simplicity and ease of implementation. With regard to the orientation representation, Euler angles, quaternion, and direction cosine matrix are common. Among them, the quaternion can arguably be considered as the most popular representation for 3D orientation estimation for its singularity-free aspect and small number of dimensions (four).

Accordingly, this paper introduces a quaternion-based CF with constraint-combined correction equations. Specifically, the proposed method improves the yaw estimation performance by combining the kinematic constraint with the conventional method introduced in [10]. In addition, the proposed CF is constructed so as to adapt to magnetic environments and optimally deal with the magnetic disturbance by adjusting the weight of the constraint with respect to the magnetometer signals, in accordance with the magnetic disturbance. The proposed method is experimentally verified using a two-link system connected by a spherical joint under different conditions of external acceleration and magnetic disturbance.

2. METHOD

2.1 Quaternion kinematics

The proposed complementary filter (CF) is expressed through the quaternion. The orientation of the sensor frame *s* with respect to the inertial frame *I* is defined as $\mathbf{q}_s = \begin{bmatrix} q_{s,0} & q_{s,1} & q_{s,2} & q_{s,3} \end{bmatrix}^T$, where $q_{s,0}$ and $[q_{s,1}, q_{s,2}, q_{s,3}]^T$ are the scalar and vector parts of the quaternion. The observation frame of an arbitrary vector $\mathbf{x} = \begin{bmatrix} x_1 & x_2 & x_3 \end{bmatrix}^T$ is transformed from the sensor frame *s* to the inertial frame *I* using $\mathbf{q}_s$ as

$$ {}^{I}\mathbf{x} = C(\mathbf{q}_s)\,{}^{s}\mathbf{x}, \tag{1} $$

where $C(\mathbf{q}_s)$ is the rotation matrix corresponding to the quaternion $\mathbf{q}_s$. The matrix $C(\mathbf{q})$ corresponding to $\mathbf{q} = \begin{bmatrix} q_0 & q_1 & q_2 & q_3 \end{bmatrix}^T$ is

$$ C(\mathbf{q}) = \begin{bmatrix} q_0^2 + q_1^2 - q_2^2 - q_3^2 & 2(q_1 q_2 - q_0 q_3) & 2(q_1 q_3 - q_0 q_2) \\ 2(q_1 q_2 - q_0 q_3) & q_0^2 - q_1^2 + q_2^2 - q_3^2 & 2(q_2 q_3 - q_0 q_1) \\ 2(q_1 q_3 + q_0 q_2) & 2(q_2 q_3 - q_0 q_1) & q_0^2 - q_1^2 - q_2^2 + q_3^2 \end{bmatrix}. \tag{2} $$

The derivative of the quaternion $\dot{\mathbf{q}}_s$ can be expressed by angular velocities ${}^{s}\boldsymbol{\omega} = \begin{bmatrix} {}^{s}\omega_x & {}^{s}\omega_y & {}^{s}\omega_z \end{bmatrix}^T$ and $\mathbf{q}_s$ as:

$$ \dot{\mathbf{q}}_s = \frac{1}{2}\mathbf{q}_s \otimes \begin{bmatrix} 0 & {}^{s}\omega_x & {}^{s}\omega_y & {}^{s}\omega_z \end{bmatrix}^T, \tag{3} $$

where $\otimes$ indicates a quaternion product.

2.2 Error modeling

The proposed method is based on a two-link system consisting of links *i* and *j*. Assume that the sensor frame coincides with link frame where the sensor is attached to the link, i.e., $s \in \{i, j\}$. The proposed method estimates the 3D orientation of link *i* within the given reference orientation of link *j*.

The normalized gravity vector $\mathbf{u}$ is

$$ \mathbf{u} = \frac{{}^{I}\mathbf{g}}{\left\| {}^{I}\mathbf{g} \right\|} = \begin{bmatrix} u_1 & u_2 & u_3 \end{bmatrix}^T, \tag{4} $$

where ${}^{I}\mathbf{g}$ is the constant gravity vector with respect to the inertial frame. A normalized geomagnetic field vector $\mathbf{n}$ is

$$ \mathbf{n} = \frac{{}^{I}\mathbf{m}}{\left\| {}^{I}\mathbf{m} \right\|} = \begin{bmatrix} n_1 & n_2 & n_3 \end{bmatrix}^T, \tag{5} $$

where ${}^{I}\mathbf{m}$ is the geomagnetic field vector with respect to the inertial frame and is constant in the local area.

The normalized gravity vector and geomagnetic field vector shown in Eqs. (4) and (5) can be rewritten as follows by combining the orientation $\mathbf{q}_i$ with the accelerometer signal ${}^{S}\mathbf{y}_A$ and the magnetometer signal ${}^{S}\mathbf{y}_M$, respectively:

$$ \hat{\mathbf{u}} = \begin{bmatrix} \hat{u}_1 & \hat{u}_2 & \hat{u}_3 \end{bmatrix}^T = C(\mathbf{q}_i) \frac{{}^{i}\mathbf{y}_A}{\left\| {}^{i}\mathbf{y}_A \right\|}, \tag{6} $$

$$ \hat{\mathbf{n}} = \begin{bmatrix} \hat{n}_1 & \hat{n}_2 & \hat{n}_3 \end{bmatrix}^T = C(\mathbf{q}_i) \frac{{}^{i}\mathbf{y}_M}{\left\| {}^{i}\mathbf{y}_M \right\|}, \tag{7} $$

where $\hat{}$ indicates that the corresponding vector is calculated from the sensor signal. In an ideal condition, in which there is no sensor noise, external acceleration, or magnetic disturbance, $\hat{\mathbf{u}}$ and $\hat{\mathbf{n}}$ obtained from the sensor signals coincide with $\mathbf{u}$ and $\mathbf{n}$, respectively.

In the conventional method [10], the error model is constructed based on the accelerometer and magnetometer signals. The proposed method combines a kinematic constraint with the conventional error model. The constraint is that, in the two-link system connected by a spherical joint, the accelerations of the joint center from each links are equal.

$$ {}^{I}\mathbf{a}_i + C(\mathbf{q}_i)\left\{\left({}^{i}\tilde{\dot{\boldsymbol{\omega}}}_i + {}^{i}\tilde{\boldsymbol{\omega}}_i\,{}^{i}\tilde{\boldsymbol{\omega}}_i\right){}^{i}\mathbf{r}_i\right\} = {}^{I}\mathbf{a}_j + C(\mathbf{q}_j)\left\{\left({}^{j}\tilde{\dot{\boldsymbol{\omega}}}_j + {}^{j}\tilde{\boldsymbol{\omega}}_j\,{}^{j}\tilde{\boldsymbol{\omega}}_j\right){}^{j}\mathbf{r}_j\right\}, \tag{8} $$

where ${}^{I}\mathbf{a}_s$ is the external acceleration of the sensor with respect to inertial frame, ${}^{s}\mathbf{r}_s$ is a constant position vector from the sensor to the joint center with respect to the sensor frame and is obtained through a calibration procedure before measurement, ${}^{s}\boldsymbol{\omega}_s$ is the angular velocity of the sensor with respect to the sensor frame, and $\tilde{}$ indicates the cross-product matrix of the vector. Equation (8) can be rewritten as Eq. (9) by expressing $\mathbf{a}$ and $\boldsymbol{\omega}$ using the accelerometer signal $\mathbf{y}_A$ and the gyroscope signal $\mathbf{y}_G$, respectively.

$$ C(\mathbf{q}_i)\mathbf{h}_i = C(\mathbf{q}_j)\mathbf{h}_j, \tag{9} $$

where $\mathbf{h}_s = {}^{s}\mathbf{y}_{A,s} + \left({}^{s}\tilde{\dot{\mathbf{y}}}_{G,s} + {}^{s}\tilde{\mathbf{y}}_{G,s}\,{}^{s}\tilde{\mathbf{y}}_{G,s}\right){}^{s}\mathbf{r}_s$. Note that the accelerometer signal $\mathbf{y}_A$ of the two links includes both the external acceleration $\mathbf{a}$ and gravity $\mathbf{g}$. However, the gravity components located on both sides cancel each other out when the gravity is expressed with respect to the inertial frame.

Let us define the normalizations of the left and right sides of Eq. (9) as $\mathbf{p} = [p_1 \quad p_2 \quad p_3]^T$ and $\hat{\mathbf{p}} = [\hat{p}_1 \quad \hat{p}_2 \quad \hat{p}_3]^T$, respectively. Then, we may set the reference vector $\mathbf{f}_0$ composed of $\mathbf{u}$, $\mathbf{n}$, and $\mathbf{p}$, and the estimation vector $\mathbf{f}$ composed of $\hat{\mathbf{u}}$, $\hat{\mathbf{n}}$, and $\hat{\mathbf{p}}$, where $\mathbf{f}$ is the function of $\mathbf{q}_i$, i.e., $\mathbf{f} = \mathbf{f}(\mathbf{q}_i)$, as follows:

$$ \mathbf{f}_0 = [u_1 \quad u_2 \quad u_3 \quad n_1 \quad n_2 \quad n_3 \quad p_1 \quad p_2 \quad p_3]^T, \tag{10} $$

$$ \mathbf{f}(\mathbf{q}_i) = [\hat{u}_1 \quad \hat{u}_2 \quad \hat{u}_3 \quad \hat{n}_1 \quad \hat{n}_2 \quad \hat{n}_3 \quad \hat{p}_1 \quad \hat{p}_2 \quad \hat{p}_3]^T. \tag{11} $$

The difference between $\mathbf{f}_0$ and $\mathbf{f}(\mathbf{q}_i)$ is defined as an error vector $\boldsymbol{\varepsilon}(\mathbf{q}_i)$.

$$ \boldsymbol{\varepsilon}(\mathbf{q}_i) = \mathbf{f}_0 - \mathbf{f}(\mathbf{q}_i) \tag{12} $$

2.3 Constraint-combined adaptive complementary filter

Set the objective function $\Phi(\mathbf{q}_i)$ to minimize the square of the error vector $\boldsymbol{\varepsilon}(\mathbf{q}_i)$ defined in Sec. 2.2.

$$ \Phi(\mathbf{q}_i) = \boldsymbol{\varepsilon}^T(\mathbf{q}_i)\boldsymbol{\varepsilon}(\mathbf{q}_i) \tag{13} $$

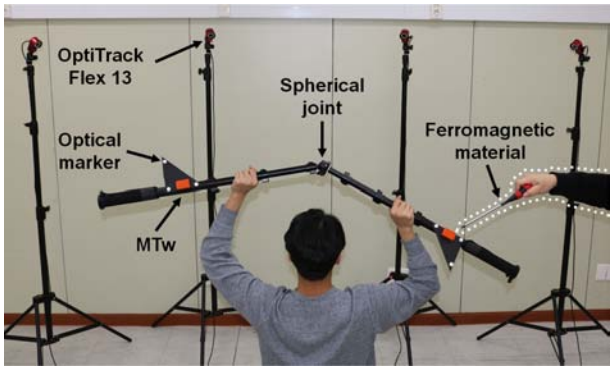

Fig. 1. Experimental setup.

To minimize the objective function $\Phi(\mathbf{q}_i)$, the proposed method calculates the incremental $\Delta\mathbf{q}_i$ from the Gauss-Newton method as follows:

$$ \Delta\mathbf{q}_i = -\left[\mathbf{J}^T\mathbf{W}\mathbf{J}\right]^{-1}\mathbf{J}^T\mathbf{W}\boldsymbol{\varepsilon}(\mathbf{q}_i), \tag{14} $$

where $\mathbf{J}$ is the Jacobian of $\boldsymbol{\varepsilon}(\mathbf{q}_i)$, which is defined as $\partial\boldsymbol{\varepsilon}(\mathbf{q}_i)/\partial\mathbf{q}_i$; and $\mathbf{W}$ is a weight matrix adjusting the weight of the kinematic constraint w relative to that of the magnetometer signal, in accordance with magnetic disturbance, as follows:

$$ \mathbf{W} = \begin{bmatrix} \mathbf{I}_3 & 0 & 0 \\ 0 & (1-w)\mathbf{I}_3 & 0 \\ 0 & 0 & w\mathbf{I}_3 \end{bmatrix}, \tag{15} $$

$$ w = \begin{cases} \dfrac{1}{th_1}\left\| {}^{I}\hat{\mathbf{m}} - {}^{I}\mathbf{m} \right\| & , \ if \ \left\| {}^{I}\hat{\mathbf{m}} - {}^{I}\mathbf{m} \right\| < th_1 \\ 1 & , \ otherwise \end{cases}. \tag{16} $$

In Eq. (16), th_1 is the threshold for magnetic disturbance. Further, when the magnetic disturbance is higher than th_1, the weight w is set to 1, and thus $\Delta\mathbf{q}_i$ is calculated using the accelerometer-related equation and the constraint equation but without the magnetometer-related equation.

Once the incremental $\Delta\mathbf{q}_i$ is obtained, the quaternion of the current step t is estimated as follows:

$$ \mathbf{q}_{i,t} = \mathbf{q}_{i,t-1} + \dot{\mathbf{q}}_{i,t-1}\Delta t + k\Delta\mathbf{q}_{i,t}\Delta t, \tag{17} $$

where the gain k is determined based on the weight w and the magnitude of $\Delta\mathbf{q}_i$ and also by considering the case where $\|\Delta\mathbf{q}_i\|$ is abnormally large, as follows:

$$ k = \begin{cases} k_{\max} & , \ if \ w < th_2 \\ k_{\max} - \dfrac{k_{\max} - k_{\min}}{th_3}\|\Delta\mathbf{q}_i\| & , \ if \ w > th_2 \cap \|\Delta\mathbf{q}_i\| < th_3 \\ k_{\min} & , \ if \ w > th_2 \cap th_3 < \|\Delta\mathbf{q}_i\| < 10 \\ 0 & , \ otherwise \end{cases}. \tag{18} $$

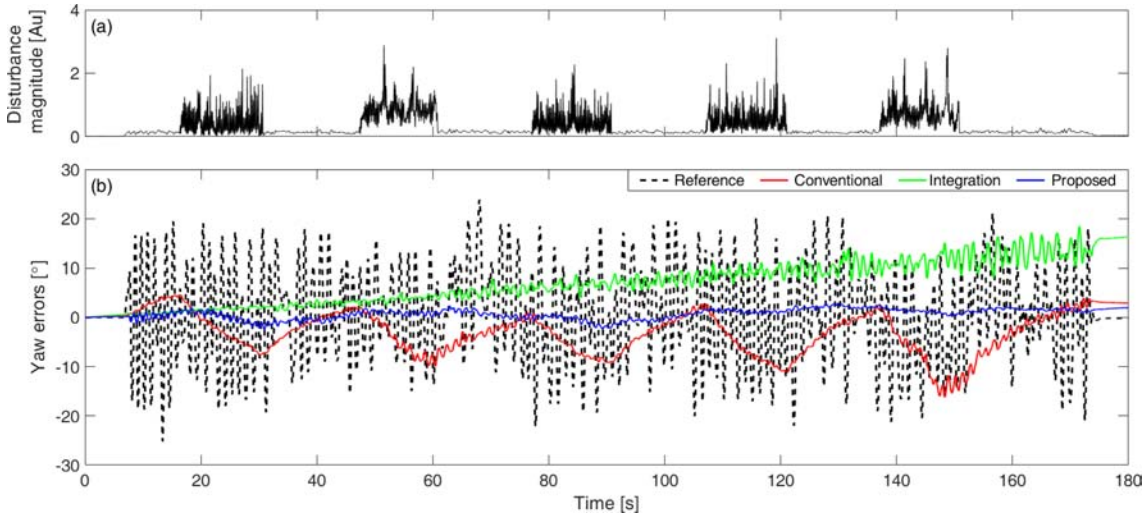

Fig. 2. Experimental result of Test 2: (a) magnitude of the applied magnetic disturbance and (b) yaw estimation errors with respect to the reference.

In Eq. (18), th_2 and th_3 are the thresholds for the weight and magnitude of $\Delta\mathbf{q}_i$, respectively. Finally, $\mathbf{q}_{i,t}$ is normalized as the quaternion expressing the orientation is a unit quaternion. Note that the quaternion update in Eq. (17) is performed only once without additional iteration.

3. RESULT

3.1 Validation experiment

To verify the proposed CF, we used MTw IMMUs (from Xsens Technologies B. V.) providing the input to the proposed CF as well as the OptiTrack Flex 13 optical motion-capture system (from Natural-Point, Inc.) as a reference system. We used a two-link system connected by a spherical joint to provide the kinematic constraint and a magnetic screw driver to apply magnetic disturbances (see Fig. 1). The constant vectors from the sensor to the joint center were estimated by the method introduced in [20], as follows: ${}^{i}\mathbf{r}_i = [51.2 \quad 0.3 \quad -2.5]^T$ *cm* and ${}^{i}\mathbf{r}_i = [50.6 \quad 0.1 \quad -2.9]^T$ *cm*.

The thresholds and parameters, such as $k_{\min}$ and $k_{\max}$, are determined using the covariance matrix adaptation evolution strategy (CMA-ES) [21] which is a genetic algorithm-based optimization method as follows: $th_1 = 0.15$, $th_2 = 0.25$, $th_3 = 0.2$, $k_{\min} = 0.01$, and $k_{\max} = 0.2$. To provide severe conditions, we added an arbitrary bias to the gyroscope signal so that a drift error occurs easily in a short experimental time, and the bias used was $b_{gyro} = [1.4 \quad 1.4 \quad 1.6]^T \times 10^{-3}$ rad/s.

Three experiments with magnetic disturbance were conducted for the validation. Tests 1 and 2 differed in acceleration condition but had a similar magnetic disturbance, whereas Tests 2 and 3 differed in magnetic disturbance but had a similar acceleration condition (see Table 1). The orientation of link *j* was given from the reference system, Flex13. For the verification, the strapdown integration method based only on gyroscope signals and the conventional method [10] without a kinematic constraint were selected for comparison. We compared the root mean square errors (RMSE) of the roll, pitch, and yaw of the proposed method

Table 1. Experimental conditions of each test.

	Average of external acceleration	Number of magnetic disturbances	Duration of magnetic disturbance
Test 1	0.9 m/s^2	5 times	15 s
Test 2	2.0 m/s^2	5 times	15 s
Test 3	1.9 m/s^2	once	30 s

Table 2. Experimental results (unit: degree).

	Method	Roll	Pitch	Yaw	Avg.
Test 1	Integration	9.01	8.30	8.27	8.53
	Conventional	3.27	3.28	6.69	4.41
	Proposed	0.81	1.25	1.16	1.07
Test 2	Integration	9.39	7.42	8.49	8.44
	Conventional	2.65	4.06	5.23	3.98
	Proposed	0.95	1.20	1.29	1.14
Test 3	Integration	5.28	5.85	5.96	5.69
	Conventional	1.69	1.72	14.73	6.04
	Proposed	1.53	0.76	1.65	1.31

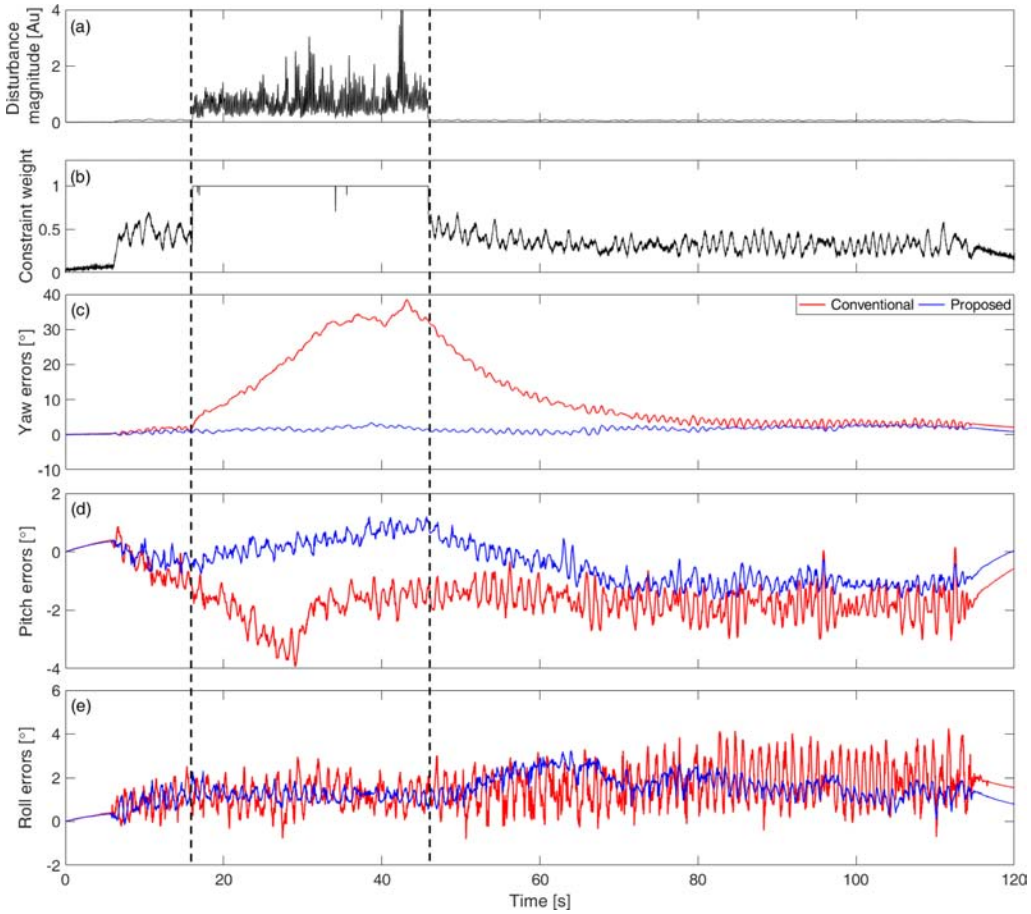

Fig. 3. Experimental result of Test 3: (a) magnitude of the applied magnetic disturbance, (b) the weight of constraint, and (c)~(e) yaw, pitch and roll estimation errors with respect to the reference, respectively.

with those from the comparison methods.

3.2 Results and discussion

Table 2 shows the RMSEs for the roll, pitch and yaw estimations from the three methods. In the low acceleration test (Test 1), the yaw estimation errors from the comparison methods were greater than 5°, while that from the proposed method was only 1.16°. In addition, the roll and pitch errors of the proposed method were 0.81° and 1.25°, respectively, which were lower than those from the comparison methods.

Figure 2 shows the yaw estimation error results in Test 2 with the applied magnetic disturbance. Au is the dimensionless arbitrary unit, and the magnitude of magnetic field at the manufacturer of MTw, Xsens, is 1. In the case of the conventional method, the yaw estimation error immediately increased when the magnetic disturbance was applied, and decreased when the disturbance disappeared. This implies that the conventional method is highly affected by the surrounding or applied magnetic environments. In contrast, in the case of the proposed method, the yaw estimation error hardly increased although the magnetic disturbance was applied, showing the robustness of the proposed method against the magnetic disturbance.

The proposed method utilizes the acceleration-level kinematic constraint, i.e., the acceleration vector at the joint center should be identical in the inertial frame, no matter from which IMU (attached to link *i* or link *j*) it is calculated. Therefore, it was expected that the constraint might not properly work at slow movements. In this regard, results of Test 1 could be compared with those of Test 2 which was a higher acceleration experiment than Test 1, with the similar magnetic disturbances applied in Test 1. Unexpectedly, the errors were mostly equivalent in Test 1 and Test 2. Accordingly, we may think that when the average external acceleration is 0.9 m/s^2 or more, the difference in estimation performance depending on the external acceleration level is not distinct.

As shown in Fig. 3, Test 3 experienced a similar acceleration condition to that of Test 2, but a much longer duration of magnetic

disturbance than Tests 1 and 2 (i.e., 30 s). The conventional method caused a significant increase in the yaw estimation error (up to almost 40°) due to the long-term magnetic disturbance. Furthermore, the pitch error increased as the magnetic disturbance was applied. This is because both the conventional and proposed methods are based on the quaternion representation.

In the proposed method, the weight of the constraint w is also shown in Fig. 3. It can be found that the weight of the constraint mostly stayed at 1 during the period of 15-45 s when the magnetic disturbance was applied. This means that, if a severe magnetic disturbance is applied, the proposed method estimates the quaternion without using the magnetometer signals. As a result, the proposed method was robust against the magnetic disturbance. Even when the magnetic disturbance from the screw driver was not applied, the magnetic condition of the laboratory where the tests were performed was not completely homogeneous, and thus, a magnetic disturbance of about 0.07 Au (arbitrary unit) was observed. Figures 3 (d) and (e) show that the addition of the constraint to the error model contributes positively to not only the yaw estimation but also the roll and pitch estimations.

4. CONCLUSIONS

This paper introduces a quaternion-based complementary filter with constraint-combined correction equations. Furthermore, the weight of the constraint relative to the magnetometer signal is adjusted to adapt to magnetic environments to optimally deal with the magnetic disturbance.

In the results of the validation experiments, the average and maximum of yaw errors were 1.17° and 1.65° from the proposed CF, respectively, and 8.88° and 14.73° from the conventional CF, respectively, showing the superiority of the proposed approach. While the constraint-combined proposed method has the effect of mainly improving the yaw estimation, the method also contributed positively to the roll and pitch estimation performance as the method is based on the quaternion representation.

However, the constraint used in the proposed method is based on the acceleration of the joint center, and thus, only works under dynamic conditions. Therefore, if magnetic disturbances are applied under static conditions, the estimation error cannot be corrected by the constraint. Another limitation of the current study might have been the use of the reference orientation for one link (link j) of the two-link system. In future work, the proposed method needs to be improved so that the orientations of both links can be estimated through the method.

ACKNOWLEDGMENT

This work was supported by a research grant from Hankyong National University for an academic exchange program in 2018.

REFERENCES

[1] A. Filippeschi, N. Schmitz, M. Miezal, G. Bleser, E. Ruffaldi, and D. Stricker, “Survey of motion tracking methods based on inertial sensors: A focus on upper limb human motion”, *Sensors*, Vol. 17, No. 6, p. 1257, 2017.

[2] Y. J. Hwang and S. B. Choi, “Vehicle orientation estimation by using magnetometer and inertial sensors”, *Trans. KSAE*, Vol. 24, No. 4, pp. 408-415, 2016.

[3] J. Chardonnens, J. Favre, F. Cuendet, G. Gremion, and K. Aminian, “A system to measure the kinematics during the entire ski jump sequence using inertial sensors”, *J. Biomech*, Vol. 46, No. 1, pp. 56-62, 2013.

[4] S. Han and J. Wang, “A novel method to integrate IMU and magnetometers in attitude and heading reference systems”, *J. Navig.*, Vol. 64, No. 4, pp. 727-738, 2011.

[5] D. Gebre-Egziabher, G. H. Elkaim, J. D. Powell, and B. W. Parkinson, “A gyro-free quaternion-based attitude determination system suitable for implementation using low cost sensors”, *Proc. of IEEE Posit. Locat. Navig. Symp.*, pp. 185-192, San Diego, CA, USA, 2000.

[6] P. H. Veltink, H. J. Bussmann, W. de Vries, W. J. Martens, and R. C. Van Lummel, “Detection of static and dynamic activities using uniaxial accelerometers”, *IEEE. Trans. Rehabil. Eng.*, Vol. 4, No. 4, pp. 375-385, 1996.

[7] G. Ligorio and A. M. Sabatini, “Dealing with magnetic disturbances in human motion capture: A survey of technique”, *Micromachines*, Vol. 7, No. 3, p. 43, 2016.

[8] C. Yi, J. Ma, H. Guo, J. Han, H. Gao, F. Jiang, and C. Yang, “Estimating three-dimensional body orientation based on an improved complementary filter for human motion tracking”, *Sensors*, Vol. 18, No. 11, p. 3765, 2018.

[9] Y. S. Suh, Y. S. Ro, and H. J. Kang, “Quaternion-based indirect Kalman filter discarding pitch and roll information contained in magnetic sensors”, *IEEE Trans. Instrum. Meas.*, Vol. 61, No. 6, pp. 1786-1792, 2012.

[10] E. R. Bachmann, I. Duman, U. Y. Usta, R. B. McGhee, X. P. Yun, and M. J. Zyda, “Orientation tracking for humans and robots using inertial sensors”, *Proc. Int. Symp. Comput. Intell. Robot. Autom.*, pp. 187-194, Monterey, CA., USA., 1999.

[11] S. O. H. Madgwick, A. J. L. Harrison, and R. Vaidyanathan, “Estimation of IMU and MARG orientation using a gradient descent algorithm”, *Proc. of IEEE Int. Conf. Rehabil. Robot.*, Zurich, Switzerland, 2011.

[12] J. K. Lee and E. J. Park, “A fast quaternion-based orientation optimizer via virtual rotation for human motion tracking”, *IEEE Trans. Biomed. Eng.*, Vol. 56, No. 8, pp. 1574-1582, 2009.

[13] G. Ligorio and A. M. Sabatini, “A linear Kalman filtering-

based approach for 3D orientation estimation from magnetic/inertial sensors", *Proc. of IEEE Int. Conf. Multisen. Fusion Integr. Intell. Syst.*, pp. 77-82, San Diego, CA, USA, 2015.

[14] J. K. Lee, "A parallel Kalman filter for estimation of magnetic disturbance and orientation", *Trans. Korean Soc. Mech. Eng. A*, Vol. 40, No. 7, pp. 659- 666, 2016.

[15] M. J. Choi and J. K. Lee, "An order-switching magnetic disturbance compensation mechanism for accurate azimuth estimation", *J. Inst. Contr. Robot. Syst*., Vol. 23, No. 7, pp. 552-558, 2017.

[16] D. Laidig, T. Schauer, and T. Seel, "Exploiting kinematic constraints to compensate magnetic disturbances when calculating joint angles of approximate hinge joints from orientation estimates of inertial sensors", *Proc. of IEEE Int. Conf. Rehabil. Robot.*, pp. 971-976, London, UK, 2017.

[17] V. Bonnet, V. Joukov, D. Kulić, P. Fraisse, N. Ramdani, and G. Venture, "Monitoring of hip and knee joint angles using a single inertial measurement unit during lower limb rehabilitation", *IEEE Sens. J.*, Vol. 16, No. 6, pp. 1557-1564, 2016.

[18] B. Fasel, J. Spörri, P. Schütz, S. Lorenzetti, and K. Aminian, "Validation of functional calibration and strap-down joint drift correction for computing 3D joint angles of knee, hip, and trunk in alpine skiing", *PloS ONE*, Vol. 12, No. 7, p. e0181446, 2017.

[19] M. J. Choi and J. K. Lee, "Inertial sensor-based attitude estimation combining a kinematic constraint for elimination of acceleration-induced inaccuracy", *Trans. Korean Soc. Mech. Eng. A*, Vol. 42, No. 3, pp. 263-269, 2018.

[20] T. Seel, T. Schauer, and J. Raisch, "Joint axis and position estimation from inertial measurement data by exploiting kinematic constraints", *Proc. of IEEE Int. Conf. on Control Appl.*, pp. 45-49, Dubrovnik, Croatia, 2012.

[21] N. Hansen, "The CMA Evolution Strategy: A Comparing Review", *in Towards a New Evolutionary Computation*, J. A. Lozano, P. Larrañaga, I. Inza, E. Bengoetxea, Eds., Springer, Berlin, pp. 75-102, 2006.